ARTICLE

N-Glycan profiling of lung adenocarcinoma in patients at different stages of disease

Erika Lattová[1] · Jana Skřičková[2] · Jitka Hausnerová[3] · Lukáš Frola[3] · Leoš Křen[3] · Ivana Ihnatová[4] ·
Zbyněk Zdráhal[1,5] · Joseph Bryant[6] · Mikuláš Popovič[6]

Abstract

Lung adenocarcinoma (LAC) is the most common form of lung cancer that increases in non-smokers at younger age. Altered protein glycosylation is one of the hallmarks of malignancy, its role in cancer progression is still poorly understood. In this study, we report mass spectrometric (MS) analysis of *N*-glycans released from fresh or defrosted tissue specimens from 24 patients with LAC. Comparison of cancerous versus adjacent healthy tissues revealed substantial differences in *N*-glycan profiles associated with disease. The significant increase in paucimannose and high-mannose glycans with 6–9 mannose residues and decline in the sialylated complex biantenary core fucosylated glycan with composition $NeuAcGal_2GlcNAc_2\text{-}Man_3GlcNAc_2Fuc$ were general features of tumors. In addition, 42 new *N*-glycan compositions were detected in cancerous tissues. The prominent changes in advanced disease stages were mostly observed in core fucosylated *N*-glycans with additional fucose (Fuc) residue/s and enhanced branching with non-galactosylated *N*-acetyl-glucosamine (GlcNAc) units. Both of these monosaccharide types were linked preferably on the 6-antenna. Importantly, as compared with noncancerous tissues, a number of these significant changes were clearly detectable early on in stage I. Application of *N*-glycan data obtained from tissues was next assessed and validated for evaluation of small sized biopsies obtained via bronchoscopy. In summary, observed alterations and data of newly detected *N*-glycans expand knowledge about the glycosylation in LAC and may contribute to research in more tailored therapies. Moreover, the results demonstrate effectiveness of the presented approach for utility in rapid discrimination of cancerous from healthy lung tissues.

✉ Erika Lattová
erika.lattova@gmail.com

✉ Jitka Hausnerová
Hausnerova.Jitka@fnbrno.cz

1 Central European Institute for Technology, Masaryk University, Kamenice 5, Brno, Czech Republic

2 Department of Respiratory Diseases and TB, University Hospital Brno and Medical Faculty of Masaryk University, Brno, Czech Republic

3 Department of Pathology, University Hospital and Medical Faculty of Masaryk University, Brno, Czech Republic

4 RECETOX, Faculty of Science, Masaryk University, Brno, Czech Republic

5 National Centre for Biomolecular Research, Faculty of Science, Masaryk University, Brno, Czech Republic

6 The Institute of Human Virology, University of Maryland, 725W. Lombard St., Baltimore, MD 21201, USA

Introduction

Lung cancer (LC) continues to be the most important cause of cancer-associated deaths worldwide [1]. The majority of LC represents non-small cell lung carcinoma (NSCLC) comprising a heterogeneous group of cancer diseases. The most common histological type of NSCLC group is LAC with an increasing trend in recent years and prevails in never smokers at younger age [2]. Importantly, LAC exhibits diverse characteristics as well, particularly at the molecular level [3]. Significant advances have been achieved in monitoring processes at biomolecular levels associated with tumorigenesis due to improvements of analytical methods [4–6]. LC studies focused on genetic alterations resulted in identification of genomic and proteomic signatures [7, 8]. Recent progress in LC detection using low-dose computed tomography (LDCT) indicates that the number of patients diagnosed in the early stages of disease will substantially increase. Notably, the vast majority of initial positive detections by LDCT are noncancerous nodules and < 5% of them are malignant,

predominantly of adenocarcinoma histology [9, 10]. The recommended treatment for patients with NSCLC at stage I is surgery. Yet, the disease recurrence in patients following this procedure is high within 5 years, up to 30% [6, 11]. Tissue-based biomarkers which can categorize patient's disease stage after surgical treatment and identify those at high-risk for recurrence could result in significant improvement [6]. Taking into consideration heterogeneity of NSCLC, broader research approaches have to be undertaken by focusing on more relevant cancer characteristics, which could effectively differentiate cancerous from indolent nodules of lung [12].

The posttranslational modification of proteins by glycosylation is critical for a variety of biological functions and its close association was also established in transformation of mammalian cells and tumor progression [13]. Glycans are generated by a set of specific enzymes, which are activated in response to intracellular and extracellular changes [14–17]. These biomolecules are typically localized on cell surfaces making them perfect targets for detection and characterization of changes during tumorigenesis [16]. Application of advanced MS technology in characterization of glycome enabled identification of specific glycans in relation with different disease processes including cancer [18–26]. Notable differences were observed in glycan expression between tumor and control tissues, as well as in expression of glycosylation related genes [27]. To date, only a few studies have been published on N-glycan analyses comparing tumor and noncancerous tissues from patients diagnosed with LAC. Satomaa et al. reported uniform expression of high-mannose glycans in both normal and malignant samples of formalin-fixed paraffin embedded (FFPE) tissues from three patient with LAC and observed increased proportion of biantennary core fucosylated N-glycan with both terminal GlcNAc residues [28]. The study of Ruhaak et al. on defrosted tissues from a large number of patients with LAC, showed increased proportion of the high-mannose and core fucosylated glycans and decreased level of galactosylation in tumor specimens [29]. Lastly, Wang et al. using FFPE tissue sections from patients, mentioned key differences in upregulation of high-mannose glycans and in downregulation of sialylated biantennary complex glycans [30]. Some discrepancies in alterations demonstrated in the above-mentioned three studies are probably due to different preparative approaches.

The main purpose of our present work was to investigate the validity of N-glycan changes in tumor and noncancerous tissues and discriminate differences related to disease stages of LAC. Previously, we reported a simple preparative procedure, which enabled effective release of all N-glycan types from freeze-dried small-sized specimens including two patient biopsies [31]. Using this approach on non-processed samples, we determined N-glycan profiles of fresh tumor versus adjacent noncancerous tissues from patients with LAC at the disease stage I–III, and evaluated

potential applicability of the data from this study to small size biopsies procured by bronchoscopy, which usually lack control (noncancerous) tissue samples.

Materials and methods

Lung tissue specimens

The tissue samples of patient cohorts were obtained through surgery and bronchoscopy from the Departments of Surgery and Respiratory Diseases and Tuberculosis, University Hospital and Faculty of Medicine, Masaryk University Brno. Tissue specimens were collected at the Department of Pathology (University Hospital and Faculty of Medicine, Masaryk University in Brno). All of the patients involved signed an informed consent approved by regional Ethics Committee. Basic demographic and clinical characteristics of patients annotated for sex, age, smoking status and histological results are listed in Supplementary Table 1. After gross morphological examination of resected lung tissues from surgery, samples were dissected from both tumor and distant noncancerous tissues and collected separately in sterile tubes. The size of these pieces varied between 5 and 10 mm. Depending on the total size of the resected lung portion, healthy tissues were cut in distances 1–5 cm from tumor and were considered as controls. To rule out a potential tumor infiltration into adjacent control tissues, histological examinations of noncancerous tissues were performed. The tubes with fresh tissues were delivered on wet ice to the proteomics laboratory. Larger tissues were cut with scissors into smaller pieces (1–3 mm), washed with cold PBS ($3 \times 300\,\mu L$) and then with distilled water ($2 \times 100\,\mu L$) to remove blood. After that, tissues were used for deglycosylation and the remaining washed pieces were stored at $-80\,^{\circ}C$.

Biopsies with sizes varying between 1 and 5 mm were obtained during examination of patients with a flexible bronchoscope and flushed into physiological solution. This solution was discarded and pieces larger than 2 mm were cut into two smaller proportions. After washing with distilled water ($3 \times 100\,\mu L$), tissue was immediately used for deglycosylation or stored at $-80\,^{\circ}C$.

N-Glycan release

Prior to deglycosylation, washed tissues were first extracted with organic solvent as described previously [31]. Briefly, 1–2 tissue pieces with size 1–3 mm were mixed with $300\,\mu L$ solution consisting of chloroform–methanol–water (8:4:1) and sonicated for 3 min, then shortly centrifuged and supernatant was discarded. The residue of organic solvent from tissue was removed by evaporation under vacuum (~10 min). Dried tissue was resuspended in 5 mM ammonium bicarbonate

solution (AB; 80 µL) with PNGase F (2 µL, Sigma-Aldrich) and vortexed at 37 °C for 2.5 h. The digest was purified or incubation continued with neuraminidase (5 mU, *Clostridium perfringens*, Sigma-Aldrich) at 37 °C for 2 h and then purified.

Solid phase extraction (SPE)

After a short centrifugation (~3 min), the liquid proportion of the digest was extracted on nonporous graphitized carbon cartridges (Supelclean™ ENVI-Carb, 1 ml Tubes). The cartridge was first washed with 100% acetonitrile (ACN), 90% ACN with 0.1% trifluoroacetic acid (TFA) following deionized water (5 × 800 µL of each solvent). Supernatant with released *N*-glycans was applied to the wet carrier, and after adsorption (5 min), the cartridge was washed with deionized water (2 × 100 µL, 5 × 600 µL) and 40% ACN (100 µL). Oligosaccharides were eluted with a solution of 40% ACN with 0.1% TFA (1 × 200 µL and 2 × 300 µL) into one tube and the eluate was evaporated.

Permethylation

SPE purified glycans were permethylated by applying a procedure reported previously [32] with slight modifications. The dried glycan pool was resuspended in DMSO (50 µL), mixed with powdered NaOH (2 mg) and MeI (15 µL). After 30 min of vortexing at room temperature, the reaction was stopped with ice-cold water (300 µL) and chloroform (300 µL). Chloroform portion was washed with distilled water until the pH of the aqueous layer was neutral and fully evaporated. Prior MS analysis permethylated glycans were reconstituted in 70% MeOH (10 µL) and 1.5 µL was added to the DHB matrix on the MALDI target.

On-target labeling with phenylhydrazine (PHN)

SPE purified glycans in deionized water (10–80 µL) underwent on-target derivatization with PHN as described previously [31, 33]. Briefly, matrix (0.8 µL) consisting of 2-aza-2-thiothymine and phenylhydrazine hydrochloride (ATT/PHN.HCl, 2:1) with the final concentration 3% in ACN/deionized water (1:1) was spotted on the surface of the AnchorChip target and followed by addition of purified glycan fraction (1.5 µL). To the wet spot, PHN labeling reagent (0.6 µL; PHN/ACN/water in ratio 1:1:4) was added and left to air dry (5–10 min).

Mass spectrometry (MS) and data analysis

MALDI-MS analysis was performed with UltrafleXtreme™ mass spectrometer (Bruker, Germany) equipped with a Smartbeam-II laser and LIFT (MS/MS) technology. All spectra were acquired in the reflectron positive mode with adjusted delay time and laser intensity 80%. The instrument was first calibrated externally using peptide calibration standards and then internally on glycans of known compositions. The spectra were obtained through the *FlexControl* software. PHN labeled *N*-glycans were identified manually and their structural assignment was derived from their molecular masses and MS/MS fragmentation patterns applying rules described previously [33, 34], supported through exoglycosidase digestion with *β-galactosidase* (bovine testes, Sigma). Fragment ions in tandem mass spectra were assigned according to the nomenclature described by Domon and Costello [35]. For annotation of detected glycan peaks and drawing their structures, the symbolic nomenclature was applied (http://www.functionalglycomics.org).

Both qualitative and quantitative comparisons of *N*-glycans were performed in non-cancerous (healthy) and tumor tissues from surgery. First, the intensities of detected glycans were evaluated for presence (nonzero intensity in a replicate) or absence otherwise. The association between presence of a glycan and sample type (tumor, healthy), sex, stage, grade, and age was assessed by Fisher's exact test or logistic regression (significance threshold $p < 0.05$). These comparisons were performed in R version 3.6.1 (https://www.R-project.org/). Secondly, the relative percentages of detected *N*-glycans were calculated from their normalized intensities after processing spectra with FlexAnalysis (Bruker) and Microsoft Excel software. To evaluate the changes between glycans of the same compositions, we define statistic $R_{T/H}$ as a ratio between intensities of tumor and paired or representative (averaged) noncancerous tissue of a patient. The ratio >1.3 or <0.8 was considered significant.

Methodology applied for clinical specimens

The validity of procedure for *N*-glycan profiling in fresh and defrosted tissues was evaluated by: (a) analyses of fresh specimens excised from tumor and noncancerous tissues (controls) from each patient subjected to surgery; and (b) repeating glycan analyses of samples from the same patient or a group of patients using defrosted tissue specimens, which were stored at −80 °C. The experiments were repeated at least three times for each tissue sample with exception of small size biopsies (<3 mm) obtained via bronchoscopy.

Results

Patients and specimens

N-Glycans of tissue specimens from 16 patients with diagnosis of LAC were subjected to comparative analysis. As listed in Supplementary Table 1, the patients included in this study were in the following disease stages and

morphological grades (G): two patients (P1 and P2) in the stage IA2-3 (G2), five patients (P3–P7) in the stage IB (G1–G3), two patients (P8 and P9) in the stage IIA (G3 and G4) and two patients (P10 and P11) in the stage IIB (both G2), five patients (P12–16) in the stage III, four of them in the stage IIIA (G2 and G3) and the last one in the stage IIIB (G3). Specimen analyzed from each patient included a tumor and a control tissue sample.

In addition, small size biopsies for glycan analyses were obtained via bronchoscopy from eight patients (Supplementary Table 1). Three of them (P17-P19) were in stage IA (G2-G3) and one patient (P20) in stage IB (G2). In the case of another four patients, clinical characteristics were as follows: in case patient P21 the stage was not determined, P22 had a chronic inflammation of lung with history of LAC and the other two patients (P23 and P24) were in stage IIIA-B/G3 and IV/G3, respectively.

## N-Glycan profiles of noncancerous tissues of LAC patients

The comparison of N-glycan profiles of noncancerous tissues adjacent to tumor before and after desialylation showed that the proportion of sialylated glycans represents between 60 and 70% and the rest were neutral forms. The presence of NeuAc residue/s was validated by analysis of permethylated pools. Figure 1 displays relative intensities of individual glycans in noncancerous tissues. There are 51 glycans that were detected in at least one technical replicate in all samples (see Supplementary Table 2).

High-mannose glycans were detected in all samples and among them only the structure with composition Man_5-$GlcNAc_2$ (m/z 1347) was observed with higher intensity (5–9%) than those carrying more mannoses (Man_{6-9} $GlcNAc_2$; < 2%). Other than differences in higher sialylation and a lower proportion of high-mannose glycans, our observations of detected glycan structures are in line with those previously reported from analyses of healthy human lungs [36]. In desialylated pools the most prevalent N-glycan (~45%) corresponded to the biantennary digalactosylated core fucosylated structure ($Gal_2GlcNAc_2Man_3GlcNAc_2Fuc$; m/z 1899). A similar glycan but without fucose (Gal_2Glc-$NAc_2Man_3GlcNAc_2$; m/z 1753) was the second major peak detected in all control lung tissues (~20%).

Tri and tetratennary core fucosylated glycans (m/z 2264, 2630), and other structures consistent with multiple LacNAc extensions (m/z 2995, 3360, 3725, 4090 etc.) were detected in all tissue specimens. The peak intensities of these glycans declined acquiring additional LacNAc unit. Among N-glycans with more Fuc residues, complex biantennary core fucosylated with the second fucose at antenna (Fuc_1-$Gal_2GlcNAc_2Man_3GlcNAc_2Fuc$; m/z 2045) was detected in all samples with highest intensity (~0.5%).

None of the glycans was significantly differentially detected in female than male in noncancerous tissues. Age was not significantly associated with presence of a glycans except for those with limited (4 out of 16) or near complete presence (13 out of 16). These glycans combined represent less than 1.40% (median 0.83%) of relative intensities of controls and more than 2.44% (median 4.16%) of relative

Fig. 1 Graphical illustration of detected N-glycans in control tissues of patients with lung adenocarcinoma with stage IB–IIIB and grade 1–4. The graph was obtained from experiments of 16 samples, which were deglycosylated and analyzed separately in different period times and represents the averaged relative intensities with error bars as shown (±SD). N-glycan compositions are on the horizontal axis (H-hexose, N-GlcNAc, F-fucose) and their percentage abundances are depicted on the vertical axis. Key symbols: Fuc (triangle), Gal (empty circle), GlcNAc (square), Man (circle). The top graph shows glycans with a range of m/z 860–1995; and the bottom one with m/z 1995–3725. For more data see Supplementary Table 2.
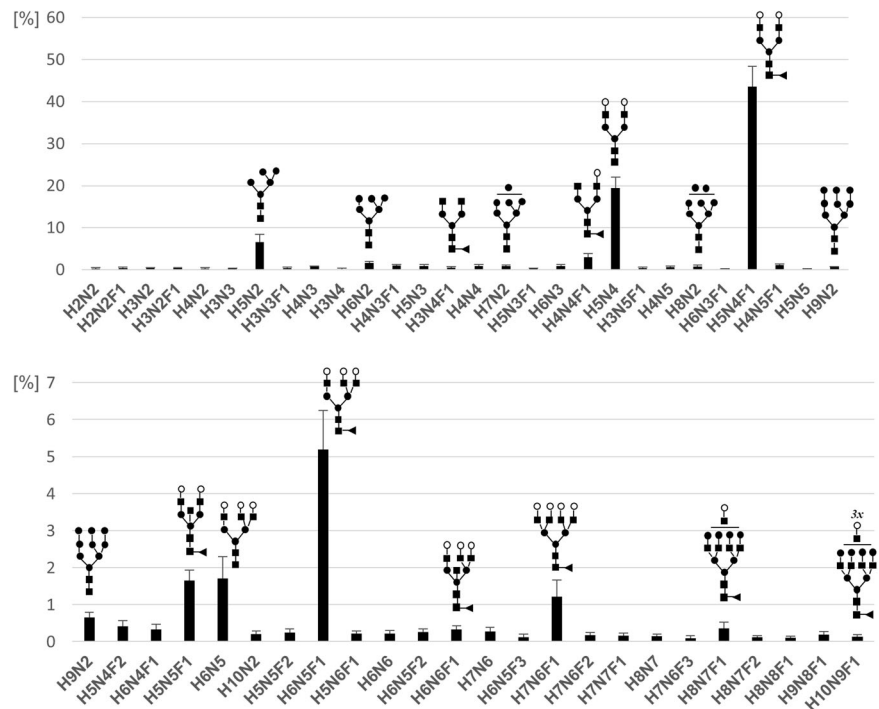
intensities of tumors. Glycan with m/z 3506.3 exhibited significantly different presence in noncancerous tissues from patients with different stage ($p = 0.012$). The glycan was dectected in all patient of stage II and III but in only 2 patients of stage I. Since, there is only one sample of grade 4 and 1, only presence of glycans in grades 2 and 3 could be evaluated. Glycan with m/z 3271.2 exhibited significantly different presence in noncancerous tissues from patients with different grade ($p = 0.041$). This glycan was detected in one out of ten samples of grade 2 and in three out of four samples of grade 3. Both glycans represent at most 0.12% (P13) and 0.06% (P16) of the total intensity of individual samples. Representative spectra of samples of different stage and grade are shown in Supplementary Figs. 1 and 2.

Despite presence of some minor glycans in noncancerous tissues of some subgroups of patients, comparison of N-glycans from control tissues adjacent to LAC tumors indicates that these profiles can be used as reference control data independent of the age, sex, stage, or grade of patients. These data could be applied in those cases when only tumor tissues are available for analyses (Fig. 1).

N-Glycan profiles of cancerous versus healthy lung tissues

MS analyses of N-glycans from cancerous tissues against control specimens showed altered glycan profiles in all patients. The extent of these alterations varied with the disease stage and histological grade of LAC. The comparison of profiles before and after incubation with neuraminidase showed that the total proportion of sialylated glycans in cancerous specimens varied in a range from 50 to 70%. An example of recorded MALDI-MS spectra of N-glycans released from tumor and healthy tissues after desialylation is illustrated in Fig. 2. The results of frequent changes in N-glycans are summarized in Supplementary Tables 2 and 3. As shown, N-glycans compositions detected in cancerous specimens were generally elevated and only some glycans (e.g., m/z 1899) declined. Importantly, 42 new asparagine-linked oligosaccharides were found exclusively or dominantly detected in cancerous tissues. Compared with control tissues, paucimannose N-glycans ($Man_{2-4}GlcNAc_2$) and their fucosylated analogs ($Man_{2-4}GlcNAc_2Fuc$) were increased in all tumors. The most significant change ($R_{T/H} > 3$), mainly in fucosylated paucimannose glycans, was observed in the patients P4 at stage IB/2 and P13 and P15 at stage III (Supplementary Table 3). Besides patient P9, high-mannose glycans with 6–9 mannose residues were increased in all cancerous tissues, Yet, the glycan with the composition $Man_5GlcNAc_2$ (m/z 1347) showed either no significant change or even decrease in majority of tumors.

The major peaks in the spectra of all analyzed lung samples after desialylation matched to the complex biantennary digalactosylated glycans with composition $Gal_2GlcNAc_2Man_3GlcNAc_2$ (m/z 1753) and a similar structure with fucose at the reducing termini—$Gal_2GlcNAc_2$-$Man_3GlcNAc_2Fuc$ (m/z 1899; e.g., Fig. 2). We observed in all tumors a consistent decrease in this core fucosylated glycan ($R_{T/H}{\sim}0.5$–0.8), while its non-fucosylated analog showed no systematic change ($R_{T/H}{\sim}0.7$–1.3). The glycan with composition $Gal_1GlcNAc_3Man_3GlcNAc_2Fuc$ (m/z 1940) showed the most prominent increase in patients P15 and P16 at stage III ($R_{T/H} > 3$). The fragmentation pattern of this glycan recorded from tumors of patients (P1–P11) at the disease stages I–IIB suggested a prevalence of the isomer with a branching on the 6-antenna (Supplementary Fig. 3a). This isomer was detected solely in all healthy tissues. However, an increase of the structure with bisecting moiety was observed in tumors of patients at the disease stage III (Supplementary Fig. 3b).

Tri- and tetra-antennary galactosylated glycans with core fucose ($Gal_{3-4}GlcNAc_{3-4}Man_3GlcNAc_2Fuc$; m/z 2264 and 2630) as well as corresponding structures branched or extended by the additional N-acetyllactosamine ($LacNAc$) units were detected in all samples (m/z 2995, 3360, 3725, 4090 etc). Comparing cancerous versus healthy tissue of patients, the increase in these glycans was noticeable mostly in the disease stage IA–IIB ($R_{T/H} {\sim}1.3$-3).

Distinctive N-glycan changes linked to disease stages of LAC

Most consistent and significant changes in N-glycan profiles at different disease stages were observed in the core fucosylated oligosaccharides carrying additional Fuc and/or non-galactosylated GlcNAc residues. An example of these changes is shown in Fig. 3 (the same spectra with m/z under 3000 are in Supplementary Fig. 4). The majority of bi-, tri-, tetra-antennary glycans with more fucoses were already detected in tumor tissues of patients at stage I, however with intensities mostly not sufficient for the structural analysis ($s/n < 5$). The stage IIB and III differed in increased occurrence of these and additional new glycans (e.g., m/z 2703, 2963, 3068, 3109, 3125, 3255, 3271, 3417, 3579). Stage III showed presence of more tetraantennary core fucosylated structures branched with one to four GlcNAc residues without further substitution besides fucose/s (e.g., 1924, 2273, 2435, 2451, 2719, 2760, 3474, 3928). Although more isomers for each of these glycans were possible, MS/MS fragmentation experiments for all of them indicated dominancy in the core fucosylated glycans with additional fucose and non-galactosylated GlcNAc residues on the 6-antenna (Supplementary Fig. 5). It should be noted, and as listed in the Supplementary Table 3, tumor tissues of mucinous LAC exhibited more heterogeneous profiles when compared with tumor tissues of LAC patients

Fig. 2 MALDI-MS spectra of N-glycans recorded from cancerous and control lung tissues of patient with LAC. In a, b are shown glycans detected in the range of m/z 860–3000; and in c, d are glycans with the range of m/z 2650–4150. The analyzed tissues are from patient P5 (IB/G2). Key symbols: Fuc (red triangle), Gal (yellow circle), GlcNAc (blue square), Man (green circle) For more peak assignments, see Supplementary Table 3.
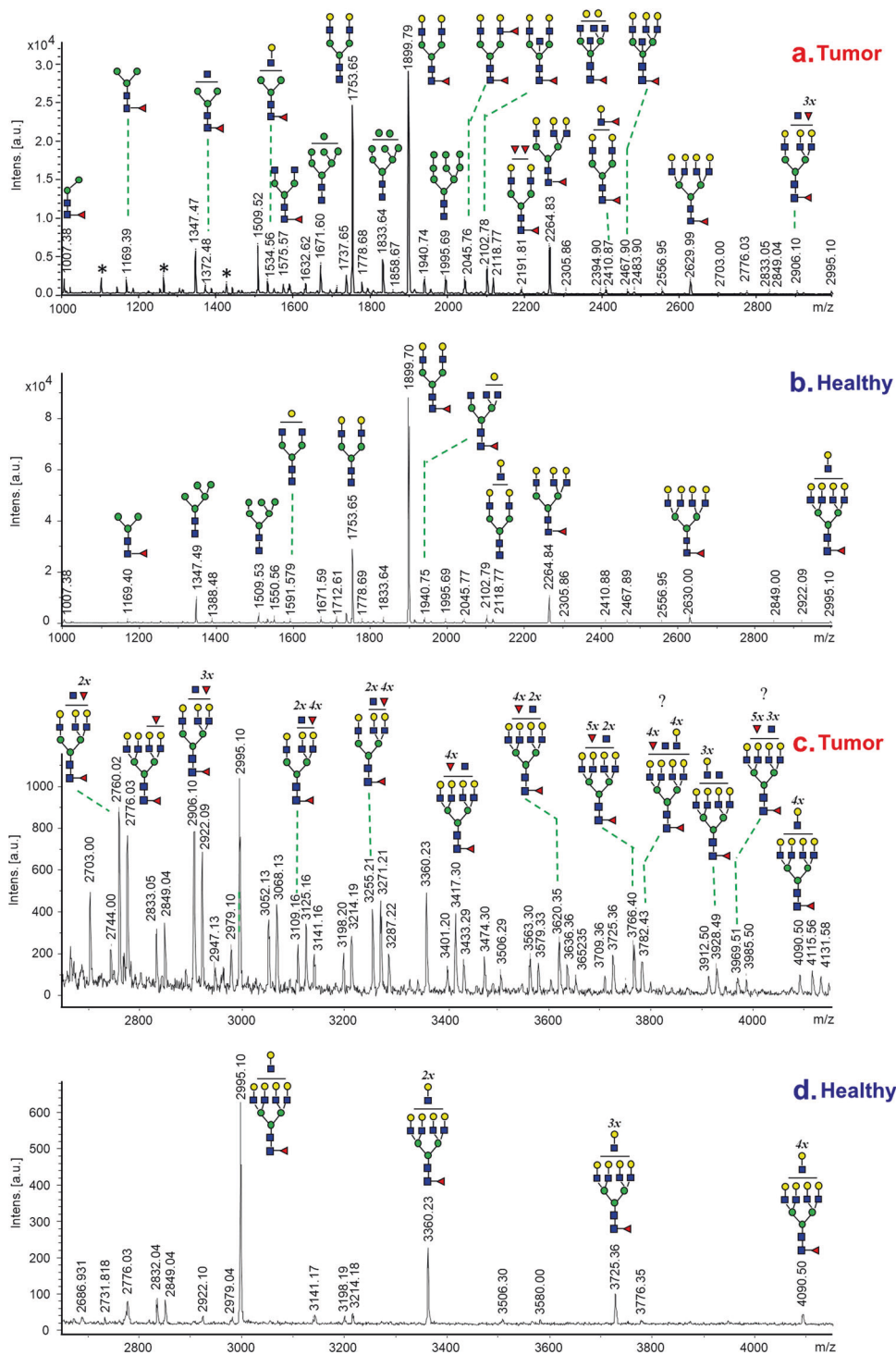
at the same disease stage. Furthermore, the N-glycan profile of cancerous tissue obtained from the patient P5 with LAC in the stage IB/G2 exhibited higher values and even more heterogeneous profile when compared with other patients with LAC (Fig. 2). This female was diagnosed with breast cancer and underwent chemotherapy seven years ago. Notably, the histological examination of regional lymph nodes did not confirm a presence of metastases in the P5 patient.

Data application for profiling of biopsies

N-Glycan profiles' data obtained from the control and cancerous tissue specimens of LAC described above were next

Fig. 3 MALDI-MS spectra with mass range 2650–4150. *N*-Glycans were obtained from malignant lung tissues of patients: **a** P3 (IB/1); **b** P9 (IIA/4); and **c** P15 (IIIA/2). All ions are MNa+. For more detailed peak assignments, see Supplementary Table 3. Glycans detected at *m/z* under 3000 in the same spectra are shown in Supplementary Figure 4.
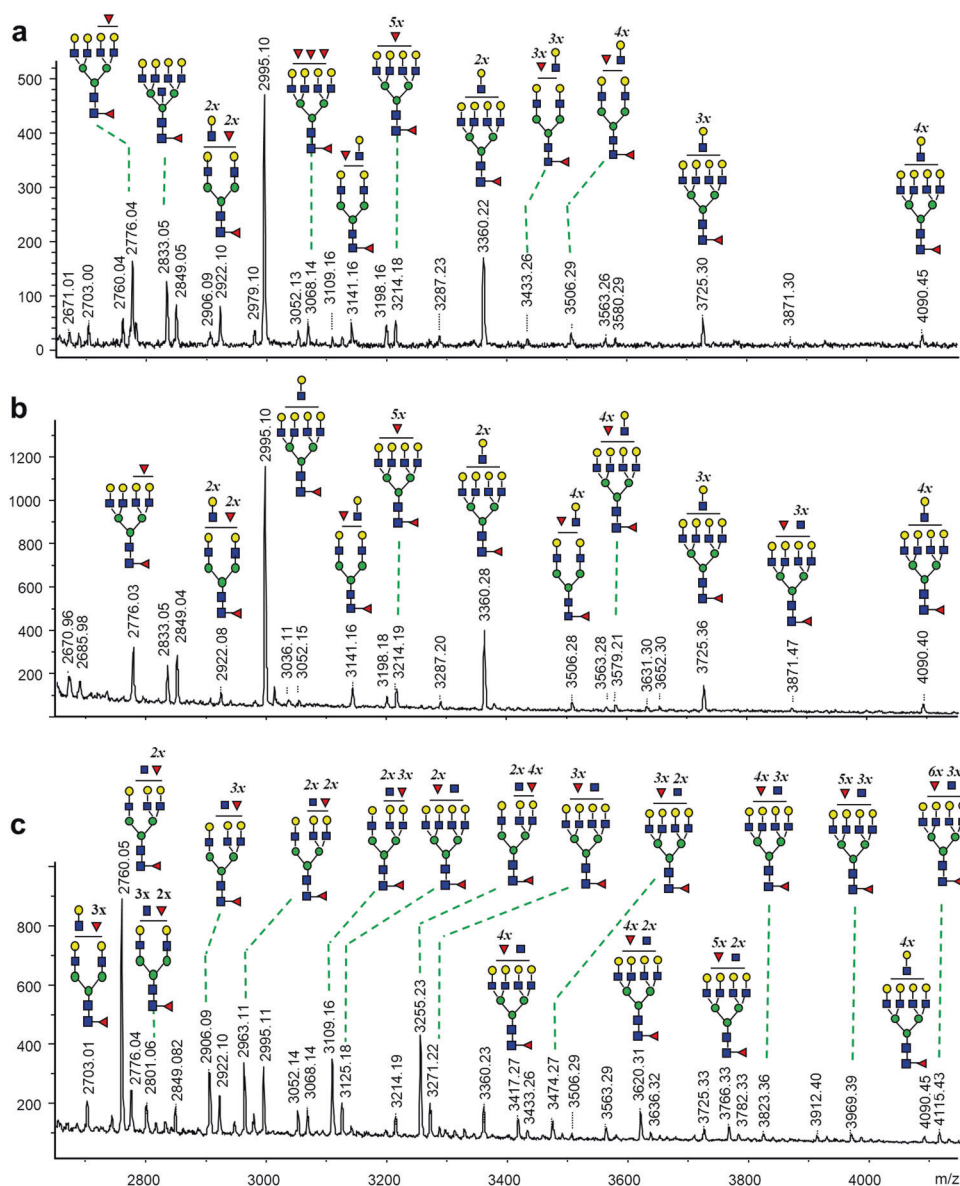

applied for evaluation of biopsies obtained during broncho-scopy examinations (Supplementary Table 1). The biopsies (~3 mm size) of three patients (P17–P19) diagnosed with LAC in stage IA3/G2 and G3, allowed detail analysis of all groups of *N*-glycans. As depicted in Fig. 4, *N*-glycan profiles of all three biopsies showed characteristics associated with disease. However, the profile of patient P17 showed resemblance to a higher stage than histology (stage IA3/2).

The sizes of biopsies (~1 mm) of patients P20 with stage IB/G2 and P21 with undetermined stage/grade allowed detection of *N*-glycan with *m/z* under 3000. On the other side, recorded profiles showed the presence of glycan structures related to malignancy (Supplementary Fig. 6).

Three other patients with diagnosis of LAC were under long-term chemotherapy and lung lesions detected in follow-up examinations suggested potential relapse (P22, P23, and P24).

In the case of patient P22, who underwent chemotherapy two years prior the bronchoscopy, the most noticeable alteration was a decline in the structure with five mannoses (*Man$_5$-GlcNAc$_2$, m/z* 1347) and biantennary digalactosylated glycan with core fucose (*Gal$_2$GlcNAc$_2$Man$_3$GlcNAc$_2$Fuc, m/z* 1899). Bi- and tri-antennary galactosylated glycans with compositions *Gal$_{2-3}$GlcNAc$_{2-3}$Man$_3$GlcNAc$_2$* (*m/z* 1753 and 2118) were significantly increased (*R$_{T/H}$* > 2; Supplementary Fig. 7). Other *N*-glycans associated only with LAC as listed for example in the Supplementary Table 3 were not detected in this biopsy. Histological examinations revealed inflammation in this biopsy and no morphological signs for malignancy. In the patients P23 and P24 in advanced stages of disease, MS analysis provided consistent data on *N*-glycan profiles up to *m/z* 2600. Despite this, *N*-glycan profiles exhibited some of changes typical for higher disease stages. In the biopsy of patient P23 at the disease

Fig. 4 Graphical illustration of detected N-glycans in the biopsies of patients P17-19 with LAC with stage IA3/G2-3 versus profile obtained from averaged values of control tissues from surgery (blue color). In **a** are glycans with a range of m/z 1007–2102; and in **b** with m/z 2102–3725.
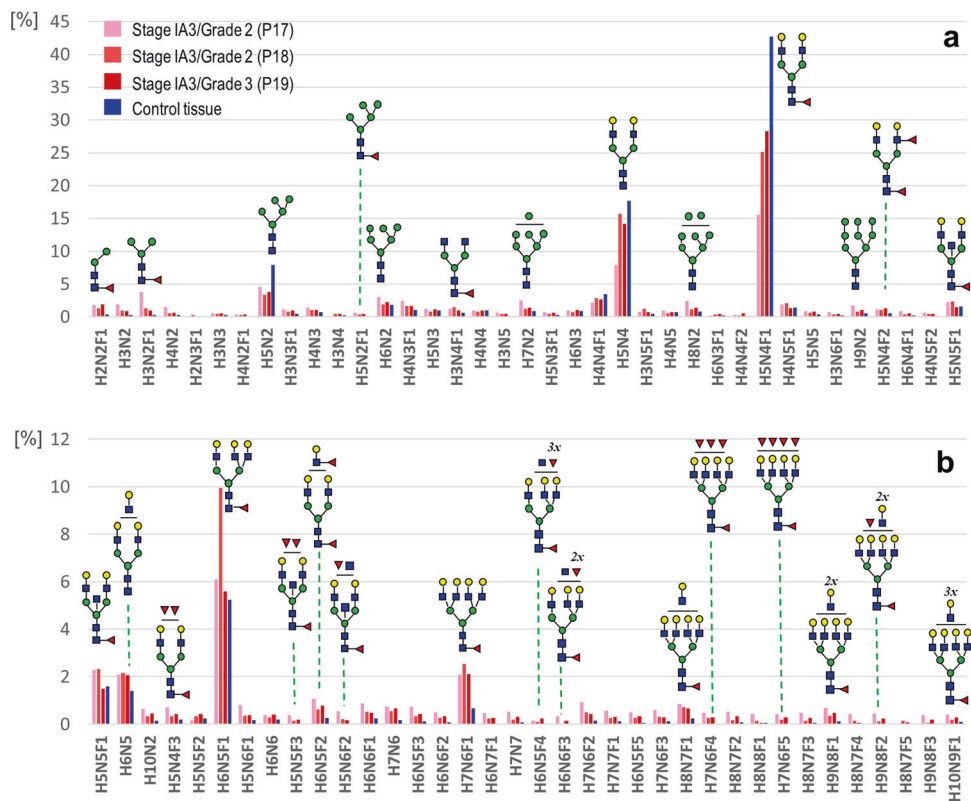
stage IIIA, besides a significant increase in structures carrying fucose residues (m/z 2045 and 2191), we observed a prominent increase in the biantennary glycan with bisecting moiety (m/z 2102, Supplementary Fig. 8a). In the P24 patient in the disease stage IV, a prominent increase was detected for tri and tetra antennary core fucosylated glycans with non-galactosylated GlcNAc residues and additional one or two fucoses on the branches—$Gal_1Fuc_1GlcNAc_3Man_3GlcNAc_2Fuc$ (m/z 2086), $Fuc_{1-2}GlcNAc_3Man_3GlcNAc_2Fuc$ (m/z 2127, 2273; Supplementary Fig. 8b). Thus, despite tissue limitations in biopsies from bronchoscopy, the application of accumulated data from glycan analyses of fresh/frozen tumor and control (non-cancerous) tissues made it possible to determine the nature of lung lesions in eight patients. The findings based on glycan detections were in line with clinical and histopathological diagnosis in these patients.

Discussion

We reported earlier sample preparative procedure for investigation of N-glycans from human cells of established cancer cell lines including those derived from LAC preserved by lyophilization [31]. The aim of the present study was to investigate applicability of this method in clinical settings for analysis of N-glycans from fresh as well as defrosted tissues of LAC patients, and to determine potential correlations between N-glycan profiles and disease

stages of LAC. The presence of sialylated glycans carrying NeuAc residue/s we confirmed by permethylation. However, comparative profiling we applied mainly on desialylated N-glycans for two reasons: (1) some minor N-glycans but of potential importance were conclusively recognized only in desialylated N-glycan pools, and (2) this approach provides benefit as a simple method for clinical utility with a high reproducibility of glycan profiles. The comparison of cancerous versus adjacent control tissues of LAC patients showed significant alteration in N-glycans in dependence to disease progressions. While noncancerous tissues of all patients provided highly consistent resemblance in glycan profiles (see Fig. 1) with few exceptions in relative intensities of glycans present in both cancerous and healthy tissues, a number of new N-glycans were detected in cancerous tissues (Supplementary Table 3). As illustrated for example by pie charts in the Supplementary Fig. 9, the clear-cut changes in proportion of some structures or grouped minor N-glycans according their compositions, were already detected in patients with LAC at stage IA and IB, which increased in patients with advanced stages.

The previous studies of LAC patients was restricted on a comparison of the same glycans detected in both cancerous and control tissues [29, 30]. Both research groups reported consistent increase in high-mannose glycans. Indeed, in our study the glycans with 6–9 mannoses were increased in all tumors (e.g., Fig. 2a). However, the glycan with composition $Man_5GlcNAc_2$ (m/z 1347) exhibited mostly a decrease.

Fig. 5 Comparison of healthy and cancerous lung tissues. In a are shown histological cross-sections of healthy and tumor lung tissues obtained from patient P9. In b is schematic illustration of main differences in glycosylation pathways of complex core fucosylated N-glycans observed between control (blue lines) and cancerous lung tissues (red lines; dotted line represents decrease) based on MS and MS/MS analyses.
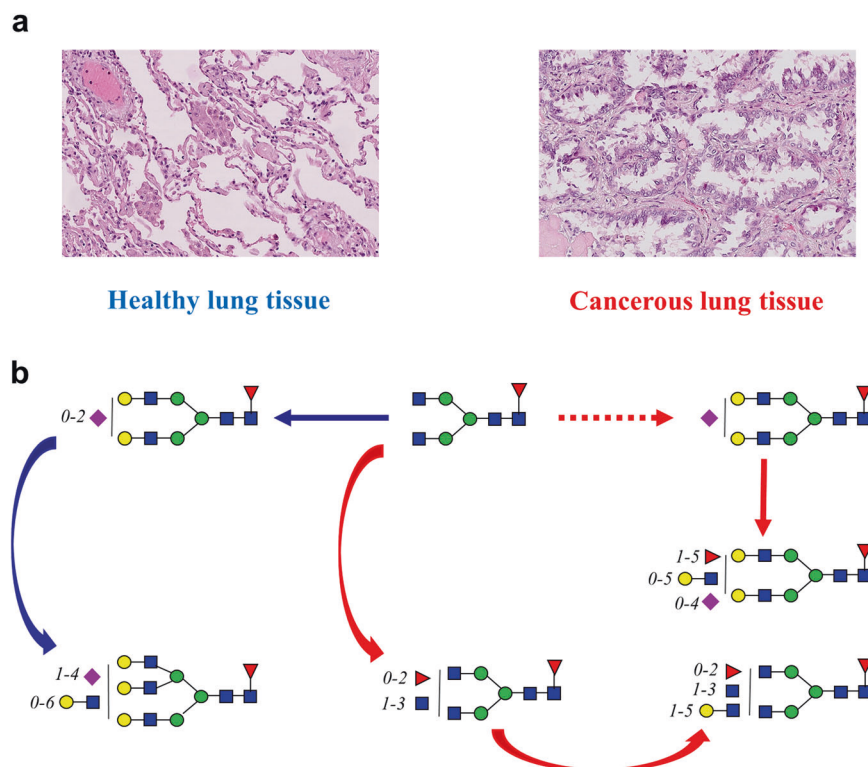
Our observation correlates with the results from recent study focused on differential expressions of the α-1,2-mannosidase genes [37]. The researcher reported that mannosidase MAN1A1 overexpression increases the high-mannose glycans with compositions $Man_{6-9}GlcNAc_2$ but not $Man_5GlcNAc_2$. Furthermore, our data obtained from analysis of control lung tissues showed that this glycan was the most significant structure among high-mannose types, whereas those with compositions $Man_{6-9}GlcNAc_2$ were detected with much lower abundances (Fig. 1).

As described previously [29], we observed a consistent decline in the sialylated complex biantennary core fucosylated digalactosylated glycan in tumors, which after desialylation was detected at m/z 1899 ($Gal_2GlcNAc_2Man_3GlcNAc_2Fuc$; e.g., Supplementary Fig. 9). However, similar glycan without fucose (m/z 1753), described also with a significant decrease in the above-mentioned study, in our tumor tissues did not show consistently the same change. On the contrary, in most tumors it was even higher than in adjacent control samples. A significant increase of this glycan was observed in one patient (P6) at a disease stage IB/2 and two patients (P8, P9) with the stages IIA/G3 and 4. The most significant increase was detected also in the biopsy of the patient P22 (Supplementary Fig. 7), suggesting its association in general with inflammation than cancer progression. It should be pointed out that some investigators emphasized the preferences for analyzing FFPE tissue sections instead of using fresh/frozen tissue specimen [30]. The main objection was that fresh or frozen tissues could contain blood, which despite thorough washing

of tissue cannot be eliminated. Surprisingly, the N-glycan profile of samples from FFPE tissue sections in their publication shows that the main glycan normally identified in blood ($NeuAc_2Gal_2GlcNAc_2Man_3GlcNAc_2$) was still the most abundant sialylated N-glycan (m/z 2792) in control FFPE tissues of permethylated samples [30]. While earlier study [36], as well as our present work (e.g., Figs. 1, 2b) shows the most abundant N-glycan in control lungs following desialylation corresponds to the core fucosylated type ($Gal_2GlcNAc_2Man_3GlcNAc_2Fuc$) which in serum/plasma is generally detected with much lower abundance either before or after desialylation.

In contrast to the previously published reports, we extended analysis into the area of new, heterogenous and more complex glycan structures. As demonstrated in the previous sections, core fucosylated glycans with multiple LacNAc extensions were detected in all spectra. These glycans dominated in mass range over 2600 Da in all control tissues and tumors with early disease stage. The core fucosylation is catalyzed by alfa-1,6-fucosyltransferase (FUT8) [38, 39]. The decline in the core fucosylated glycan, regularly observed for N-glycan with a composition $Gal_2GlcNAc_2Man_3GlcNAc_2Fuc$ (or as $NeuAc_{1-2}Gal_2GlcNAc_2Man_3GlcNAc_2Fuc$ prior to desialylation) in our work and in previous study [29], differs from the previously reported upregulation of FUT8 in NSCLC and metastasis [40]. On the other side, the most significant differences in early stages were in the increase of tri and more antennary glycans with core fucose and those carrying additional fucose/s on the antennae (Supplementary Fig. 9). Increased arm fucosylation is

most likely the result of upregulated α-1-3-fucosyltrasferase (FUT3) [26]. Very lastly, it has been reported that both FUT3 and FUT6 played key roles in mediating metastasis to bone [17]. We further observed that fucosylated glycans were often branched with non-galactosylated GlcNAc residues, preferably linked on the 6-antena at LAC higher stages (Supplementary Fig. 5). It provides evidence that besides increased activities in FUT3 and FUT6 the progression of LAC is associated also with a higher expression of GnT-V, a glycosyltransferase that catalyzes the formation of β-1,6-GlcNAc branches. Upregulation in this enzyme has been described with malignancies as well [16, 41]. The majority of newly detected N-glycans has not been reported in LAC patients in earlier studies. Moreover, 20 of them are not listed in the human or animal glycan databases. The main difference in glycosylation pathways of the core fucosylated glycans in brief is illustrated in a scheme of Fig. 5. These differences are derived based on identification asparagine-linked oligosaccharides in control and cancerous lung tissues.

Next, we tested applicability of the N-glycan data obtained in this study for evaluation of biopsies with limited sizes and lacking control tissues. Despite these limitations, the detected glycans in the biopsies of patients P17–21 showed characteristic features of malignant transformation of tissue (Fig. 4 and Supplementary Fig. 6). However, the biopsy of female (P17) in disease stage IA3/G2, showed a more heterogeneous profile than we expected for this stage. As mentioned in the section of Results, among examined cancerous tissues from surgery, female in the disease stage IB, of which MS spectra can be seen in Fig. 2, displayed profile that was much more heterogeneous then stage III. We did not include all the detected glycans from her in Supplementary Tables 2 and 3 because of patient's diagnosis of cancer in the past. However, patient P17 has no record any malignancy prior to LAC.

Three further patients (P22–24) were checked for a potential relapse of LAC. The patient P22 showed an alteration not characteristic for LAC (Supplementary Fig. 7), which was confirmed by histology examinations displaying only inflammation with no malignancy. In two other patients (P23 and P24) suspected of LAC relapse, the identified N-glycans indicated poor prognosis (Supplementary Fig. 8). The glycans at m/z 2086, 2127 and 2273 corresponded to the tri and tetra antennary structures with compositions $Gal_1Fuc_1GlcNAc_3$-$Man_3GlcNAc_2Fuc$ and $Fuc_{1-2}GlcNAc_4Man_3GlcNAc_2Fuc$ and were detected in high prevalence particularly in biopsy of the patient P24 at stage IV.

In conclusion, we present a comprehensive N-glycan analysis in tissues of LAC patients. We found a clear difference between cancerous and healthy lung tissue and the changes in N-glycan profiles are becoming more prominent in advanced stages (II and III) of disease. Data from comparative N-glycan analyses of tumor tissues to controls using either from the same patient or the reference control averaged from 16 patients showed the same significant difference between glycan profiles of tumors and noncancerous lung tissues. Potentially, these data enable expeditious differentiation between LAC and noncancerous lung tissues including those biopsy specimens, which lack controls. We found a number of adenocarcinoma-related glycan structures not reported previously in tumor tissues of LAC patients. The presented N-glycan database enables more focused follow up studies on a larger patient cohort aimed to determine potential markers in the early disease stage as well as those associated with the early metastatic processes. Moreover, this study demonstrates high potential for the approach used here in clinical testing. The analysis of N-glycans from fresh tissue provides an additional opportunity for a rapid discrimination between cancerous and healthy lung tissue. New glycan structures might serve as promising biomarkers of which presence in the first step of analysis indicates malignant processes prior to carrying out more complex, however demanding quantitative data analysis. We were able to detect unexpected abnormalities in profiles of two patients, not consistent with assigned histological stages and we observed glycans characteristic of cancerous tissue from bronchoscopy in another patient where histology was not successful. Thus, a combination of knowledge from different methodologies might together provide deeper insights into malignancy and its behavior on more individual levels.

Conflicts of interest The authors declare no potential conflicts of interest.

References

1. Torre LA, Siegel RL, Jemal A. Lung cancer statistics. In: Ahmad A, Gadgeel S, editors. Lung cancer and personalized medicine: current knowledge and therapies. Cham: Springer International Publishing, 2016. p. 1–19.
2. Hashimoto T, Tokuchi Y, Hayashi M, et al. Different subtypes of human lung adenocarcinoma caused by different etiological factors. Am J Pathol. 2000;157:2133–41.
3. Okayama H, Kohno T, Ishii Y, et al. Identification of genes upregulated in ALK-positive and EGFR/KRAS/ALK-negative lung adenocarcinomas. Cancer Res. 2012;72:100–11.
4. Cibulskis K, Lawrence MS, Carter SL, et al. Sensitive detection of somatic point mutations in impure and heterogeneous cancer samples. Nat Biotechnol. 2013;31:213–9.
5. Balani S, Nguyen LV, Eaves CJ. Modeling the process of human tumorigenesis. Nat Commun. 2017;8:15422.

6. Robles AI, Harris CC. Integration of multiple "OMIC" bio-markers: a precision medicine strategy for lung cancer. Lung Cancer. 2017;107:50–58.

7. Planck M, Edlund K, Botling J, et al. Genomic and transcriptional alterations in lung adenocarcinoma in relation to EGFR and KRAS mutation status. Plos ONE. 2013;8:e78614.

8. Network TCGAR. Comprehensive molecular profiling of lung adenocarcinoma. Nature. 2014;511:543–50.

9. Doria-Rose VP, White MC, Klabunde CN, et al. Use of lung cancer screening tests in the United States: results from the 2010 National Health Interview Survey. Cancer Epidemiol Biomark Prev. 2012;21:1049–59.

10. Team TNLSTR. Reduced lung-cancer mortality with low-dose computed tomographic screening. N Engl J Med. 2011;365:395.

11. Chansky K, Sculier J-P, Crowley JJ, et al. The International Association for the Study of Lung Cancer Staging Project: prognostic factors and pathologic TNM stage in surgically managed non-small cell lung cancer. J Thorac Oncol. 2009;4:792–801.

12. Chen Z, Fillmore CM, Hammerman PS, et al. Non-small-cell lung cancers: a heterogeneous set of diseases. Nat Rev Cancer. 2014;14:535–46.

13. Dwek RA. Glycobiology: toward understanding the function of sugars. Chem Rev. 1996;96:683–720.

14. Bertozzi CR, Kiessling LL. Chemical glycobiology. Science. 2001;291:2357–64.

15. Varki A, Cummings RD, Esko JD, et al., editors. Essentials of glycobiology, 3rd ed. Cold Spring Harbor (NY): Cold Spring Harbor Laboratory Press, 2015. http://www.ncbi.nlm.nih.gov/books/NBK310274/. Accessed 29 August 2018.

16. Taniguchi N, Kizuka Y. Glycans and cancer: role of N-glycans in cancer biomarker, progression and metastasis, and therapeutics. Adv Cancer Res. 2015;126:11–51.

17. Esposito M, Mondal N, Greco TM, et al. Bone vascular niche E-selectin induces mesenchymal–epithelial transition and Wnt activation in cancer cells to promote bone metastasis. Nat Cell Biol. 2019;21:627–39.

18. Lattová E, Tomanek B, Bartusik D, et al. N-glycomic changes in human breast carcinoma MCF-7 and T-lymphoblastoid cells after treatment with herceptin and herceptin/lipoplex. J Proteome Res. 2010;9:1533–40.

19. Mann BF, Goetz JA, House MG, et al. Glycomic and proteomic profiling of pancreatic cyst fluids identifies hyperfucosylated lactosamines on the n-linked glycans of overexpressed glycoproteins. Mol Cell Proteom. 2012;11:M111.015792.

20. Ji IJ, Hua S, Shin DH, et al. Spatially-resolved exploration of the mouse brain glycome by tissue glyco-capture (TGC) and nano-LC/MS. Anal Chem. 2015;87:2869–77.

21. Sethi MK, Thaysen-Andersen M, Smith JT, et al. Comparative N-glycan profiling of colorectal cancer cell lines reveals unique bisecting glcnac and α-2,3-linked sialic acid determinants are associated with membrane proteins of the more metastatic/aggressive cell lines. J Proteome Res. 2014;13:277–88.

22. Dahmen A-C, Fergen M-T, Laurini C, et al. Paucimannosidic glycoepitopes are functionally involved in proliferation of neural progenitor cells in the subventricular zone. Glycobiology. 2015;25:869–80.

23. Möginger U, Grunewald S, Hennig R, et al. Alterations of the human skin N- and O-glycome in basal cell carcinoma and squamous cell carcinoma. Front Oncol. 2018;8. https://doi.org/10.3389/fonc.2018.00070.

24. Arnold JN, Saldova R, Galligan MC, et al. Novel glycan biomarkers for the detection of lung cancer. J Proteome Res. 2011;10:1755–64.

25. Vasseur JA, Goetz JA, Alley WR, et al. Smoking and lung cancer-induced changes in N-glycosylation of blood serum proteins. Glycobiology. 2012;22:1684–708.

26. Pompach P, Ashline DJ, Brnakova Z, et al. Protein and site specificity of fucosylation in liver-secreted glycoproteins. J Proteome Res. 2014;13:5561–9.

27. Potapenko IO, Haakensen VD, Lüders T, et al. Glycan gene expression signatures in normal and malignant breast tissue; possible role in diagnosis and progression. Mol Oncol. 2010;4:98–118.

28. Satomaa T, Heiskanen A, Leonardsson I, et al. Analysis of the human cancer glycome identifies a novel group of tumor-associated N-acetylglucosamine glycan antigens. Cancer Res. 2009;69:5811–9.

29. Ruhaak LR, Taylor SL, Stroble C, et al. Differential N-glycosylation patterns in lung adenocarcinoma tissue. J Proteome Res. 2015;14:4538–49.

30. Wang X, Deng Z, Huang C, et al. Differential N-glycan patterns identified in lung adenocarcinoma by N-glycan profiling of formalin-fixed paraffin-embedded (FFPE) tissue sections. J Proteom. 2018;172:1–10.

31. Lattová E, Bryant J, Skřičková J, et al. Efficient procedure for N-glycan analyses and detection of endo H-like activity in human tumor specimens. J Proteome Res. 2016;15:2777–86.

32. Ciucanu I, Kerek F. A simple and rapid method for the permethylation of carbohydrates. Carbohydr Res. 1984;131:209–17.

33. Lattová E, Skřičková J, Zdráhal Z. Applicability of phenylhydrazine labeling for structural studies of fucosylated N-glycans. Anal Chem. 2019;91:7985–90.

34. Lattová E, Perreault H. The usefulness of hydrazine derivatives for mass spectrometric analysis of carbohydrates. Mass Spectrom Rev. 2013;32:366–85.

35. Domon B, Costello C. A systematic nomenclature for carbohydrate fragmentations in FAB-MS/MS spectra of glycoconjugates. Glycoconj J. 1988;5:397–409.

36. Walther T, Karamanska R, Chan RWY, et al. Glycomic analysis of human respiratory tract tissues and correlation with influenza virus infection. PLoS Pathog. 2013;9:e1003223.

37. Tu H-C, Hsiao Y-C, Yang W-Y, et al. Up-regulation of golgi α-mannosidase IA and down-regulation of golgi α-mannosidase IC activates unfolded protein response during hepatocarcinogenesis. Hepatol Commun. 2017;1:230–47.

38. Voynow JA, Kaiser RS, Scanlin TF, et al. Purification and characterization of GDP-L-fucose-N-acetyl beta-D-glucosaminide alpha 1–6fucosyltransferase from cultured human skin fibroblasts. Requirement of a specific biantennary oligosaccharide as substrate. J Biol Chem. 1991;266:21572–7.

39. Ihara H, Hanashima S, Okada T, et al. Fucosylation of chit-ooligosaccharides by human α1,6-fucosyltransferase requires a nonreducing terminal chitotriose unit as a minimal structure. Glycobiology. 2010;20:1021–33.

40. Chen C-Y, Jan Y-H, Juan Y-H, et al. Fucosyltransferase 8 as a functional regulator of nonsmall cell lung cancer. PNAS. 2013;110:630–5.

41. Lau KS, Dennis JW. N-glycans in cancer progression. Glycobiology. 2008;18:750–60.